02

Features of the Faraday and Kerr magneto-optical effects in nanoscale $Y_3Fe_5O_{12}$ films and $Gd_3Ga_5O_{12}$, $Nd_3Ga_5O_{12}$ substrates

© Yu.P. Sukhorukov[1], A.V. Telegin[1], I.D. Lobov[1], A.M. Korovin[2]

[1] M.N. Mikheev Institute of Metal Physics, Ural Branch, Russian Academy of Sciences, Yekaterinburg, Russia
[2] Ioffe Institute, St. Petersburg, Russia

e-mail: telegin@imp.uran.ru

Received May 31, 2024
Revised June 29, 2024
Accepted June 29, 2024

The Faraday and Kerr magneto-optical effects for ultra-thin films of yttrium iron garnet $Y_3Fe_5O_{12}$ and monocrystalline substrates $Gd_3Ga_5O_{12}$ and $Nd_3Ga_5O_{12}$ were studied in the visible spectrum range $1.3 < E < 4.5$ eV in fields up to 1 T. Verdet constants for the substrates $Gd_3Ga_5O_{12}$ and $Nd_3Ga_5O_{12}$ were determined, and features of the Faraday and Kerr effects spectra related to the magneto-optical properties of the substrates for $Y_3Fe_5O_{12}/Gd_3Ga_5O_{12}$ and $Y_3Fe_5O_{12}/Nd_3Ga_5O_{12}$ structures were identified. It was shown that, by excluding the contribution from the substrates, the spectral and field dependencies of the magneto-optical effects in nanoscale films correspond to the data for bulk $Y_3Fe_5O_{12}$. An estimation of the relaxation layer was carried out, and it was shown that nanoscale films, being comparable in thickness to the critical layer, can possess a specific Faraday rotation ($\sim 15-20$ deg/μm) close to that of bulk materials, demonstrating the high quality of the obtained samples.

Keywords: Faraday Effect, Kerr Effect, Magneto-optics, YIG (Yttrium Iron Garnet), Films, Interface.

DOI: 10.61011/EOS.2024.07.59646.6245-24

Introduction

The Faraday and Kerr magnetooptical (MO) effects in $Y_3Fe_5O_{12}$ (YIG) (ferrimagnetic yttrium-iron garnet) crystals and films have been studied extensively beginning from the middle of the past century and are currently used in a wide range of optoelectronic devices ([1–3] and references therein). The existing synthesis technologies are used to control the structure and composition of a material at the monoatomic level which is necessary for nanoelectronics development. Therefore, YIG films less than 100 nm in thickness and nanostructured materials based on them are of great interest. The need for nanometer-thick films (d) is explained by the reduction of optical loss ($D_Y = 10\lg[Y_{in}/Y_{out}]$, where Y_{in} and Y_{out} are the intensities of incident light and transmitted light through the film) in film-based devices. However, for successful integration with other microwave, opto- and nanolectronic planar elements, ultra-thin films should also have MO parameters close to bulk materials, weak decay of electromagnetic radiation, etc.

At the same time, it is known that at thicknesses less than 100 nm the MO properties of magnetic materials, including YIG, may vary significantly. This primarily include magnetization reduction due to influence of a film-substrate interface and film surface contributions, resonances occurring in multilayer structures, increase in the MO Q factor, etc. [1,4,5]. A special role in thin-film structures is assigned to the study of magneto-passive and so-called magneto-dead layers the total thickness of which becomes comparable with the film thickness, and to surface states ([6–8] and references therein). Moreover, for nanoscale films, the Faraday rotation and Kerr effect values become comparable with those in paramagnetic substrates in the same conditions [9–12].

Thus, when determining the MO parameters of YIG/substrate thin-film structures, problems arise that are associated with consideration of the MO contribution of substrates, determination of the film-substrate interface role, and search for conditions in which MO of nanoscale YIG films are retained as in bulk materials.

Single-crystalline ultra-thin YIG films fabricated on the $Gd_3Ga_5O_{12}$ and $Nd_3Ga_5O_{12}$ substrates creating epitaxial stresses of different sign and magnitude in the film were used to solve these problems. Features of the Faraday and Kerr effects in the fabricated thin-film YIG/$Gd_3Ga_5O_{12}$ and YIG/$Nd_3Ga_5O_{12}$ structures, YIG films and separately in the $Gd_3Ga_5O_{12}$ and $Nd_3Ga_5O_{12}$ substrates were examined. The relaxation layer size was determined and the role of substrates in formation of the Faraday and Kerr effects in the nanoscale $Y_3Fe_5O_{12}$ films was addressed.

Experimental

Samples in the form of $d = 10$ and 23 nm $Y_3Fe_5O_{12}$ films were grown by the laser molecular beam epitaxy method [13,14] on double-side-polished $d = 0.5$ mm $Gd_3Ga_5O_{12}-$GGG(111) films [15]. One $d = 20$ nm film was grown on a $Nd_3Ga_5O_{12}-$NdGG(111) substrate [16].

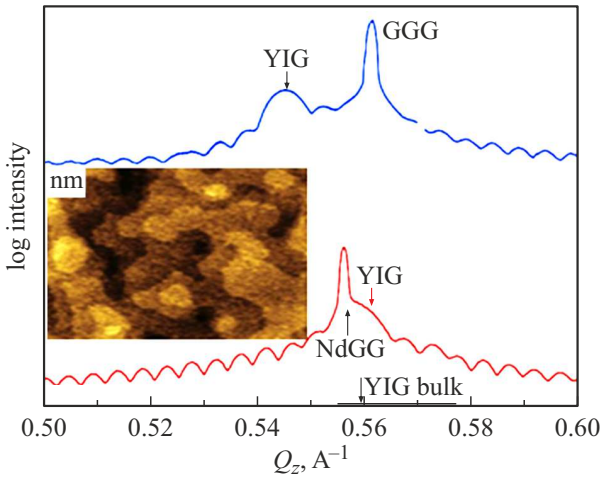

Figure 1. X-ray diffraction patterns for the YIG/GGG structures (blue line) and YIG/NdGG structures (brown line). Arrows indicate the typical peak positions for the YIG films, YIG crystal, GGG and NdGG substrates. The inset shows a magnified YIG film surface according to the ACM data.

Before the film growth, the substrates were annealed in air at $T = 1000°$C during 3 h. Substrate surface roughness in an area of $25 \times 25\,\mu$m was equal to ≤ 0.5 nm. Films were grown in a deposition chamber at $P = 10^{-5}$ Pa in oxygen atmosphere $P_O = 4$ Pa with a purity of 9.99% and at the substrate temperatures of $T_s = 650°$C and 700°C for GGG-based films and NdGG-based film, respectively. The films were deposited through the exposure of the$Y_3Fe_5O_{12}$ target to the 99.99% high purity laser with wavelength$\lambda = 248$ nm and power $P = 3$ W/cm^2.

The film growth process was controlled by the high-energy electron diffraction method. Film thickness was determined by the deposition time and X-ray data. Chemical composition of the target and films was controlled by X-ray (energy-dispersive X-ray analysis, X-ray diffraction) and electronic microscopy methods. The quality of samples is confirmed by atomically smooth film surfaces produced using an atomic-force microscope (inset in Figure 1). From the X-ray diffraction data for the YIG/NdGG and YIG/GGG structures compared with bulk YIG it follows that the films are under tension stresses at the GGG substrate interface and under compression stresses at the NdGG substrate interface (Figure 1). This corresponds to bonding forces occurring as a result of difference in crystal lattice parameters at the interface between the oriented films and substrates [4]. Synthesis and postgrowth treatment of the YIG on various substrates are described in more detail in [13–15].

The Faraday effect (f) in the structures and substrates was measured at room temperature using a grating monochromator within the energy range from 2 eV to 3.8 eV and in magnetic fields up to $H = 0.8$ T according to the single-beam modulation procedure at the angle between the quartz polarizer and analyzer $\alpha = 45°$. Considering small Faraday rotation angles in the samples, f was calculated as follows [17]

$$f = (45/\pi)(\delta I/I_0)\ [\text{deg}], \qquad (1)$$

where δI is the signal intensity variation at the photodetector with opposite magnetic field directions, I_0 is the signal intensity at the photodetector at $H = 0$ determined as $I_0 = I_{\parallel}\cos^2(\alpha)$, $I_{\parallel}$ is the signal intensity with parallel polarizer and analyzer.

The specific Faraday rotation was calculated with respect to $F = f/d\ [\text{deg}/\mu\text{m}]$.

The polar Kerr effect (φ_K) was measured on the same samples using a separate optical setup in the spectral range from 1.3 eV to 4.5 eV in fields up to $H = 1.2$ T. A standard optical scheme was used, including the DKSSh-120 W xenon lamp, grating monochromator, quartz polarizer and analyzer, sample on the electromagnet field concentrator and photoelectronic amplifier. Measurements were conducted using the modulation method with the sample remagnitized at a frequency of 2 Hz. Each measurement was started with the sample in demagnetized condition. Measurements of φ_K were conducted from the film side at the light incidence angle $\Theta = 52°$ to the magnetization of the $\mathbf{M} \parallel z$-axis coinciding with the direction of normal to the film surface and light propagation, at the$s$-polarization of the incident light and $\alpha = 45°$ (with respect to the s- and p-polarizations). Reflected light ellipticity was not determined due to the measurement and installation procedure restrictions.

The experiment recorded reflected light intensity variation that was later converted into rotation by Malus's law (on a linear segment). The measurement error was $\sim 5\%$. For ease of comparison with the literature data, the obtained values of φ_K were modifyed to the nominal ones at $\Theta = 0°$ considering $K = \varphi_K(\Theta = 0°)/\varphi_K(\Theta = 52°)$ based on the expression [1]

$$\varphi_K(\Theta) = i[N^2(\sin\Theta\,\mathrm{tg}\,\Theta + (N^2 - \sin^2\Theta)^{0.5})]Q/$$
$$[(N^2 - 1)(N^2 - \mathrm{tg}^2\,\Theta)], \qquad (2)$$

where N is the refractive index of YIG or GGG, NGG (whilst the refractive index of air was assumed equal to 1), and Q is the MO Voigt parameter.

$1/K$ was equal to 0.592 for the YIG/GGG and YIG/NdGG film structures and 0.544 for the GGG and NGG substrates.

Faraday effect in the GGG, NGG substrates and YIG films

As mentioned in the introduction, formation of the film-substrate interface leads to emergence of a relaxation layer [6] that may significantly affect the magnetic properties and accordingly the Faraday and Kerr effects in the ultra-thin YIG films. To determine the role of the interface in formation of the MO properties of nanoscale films, two

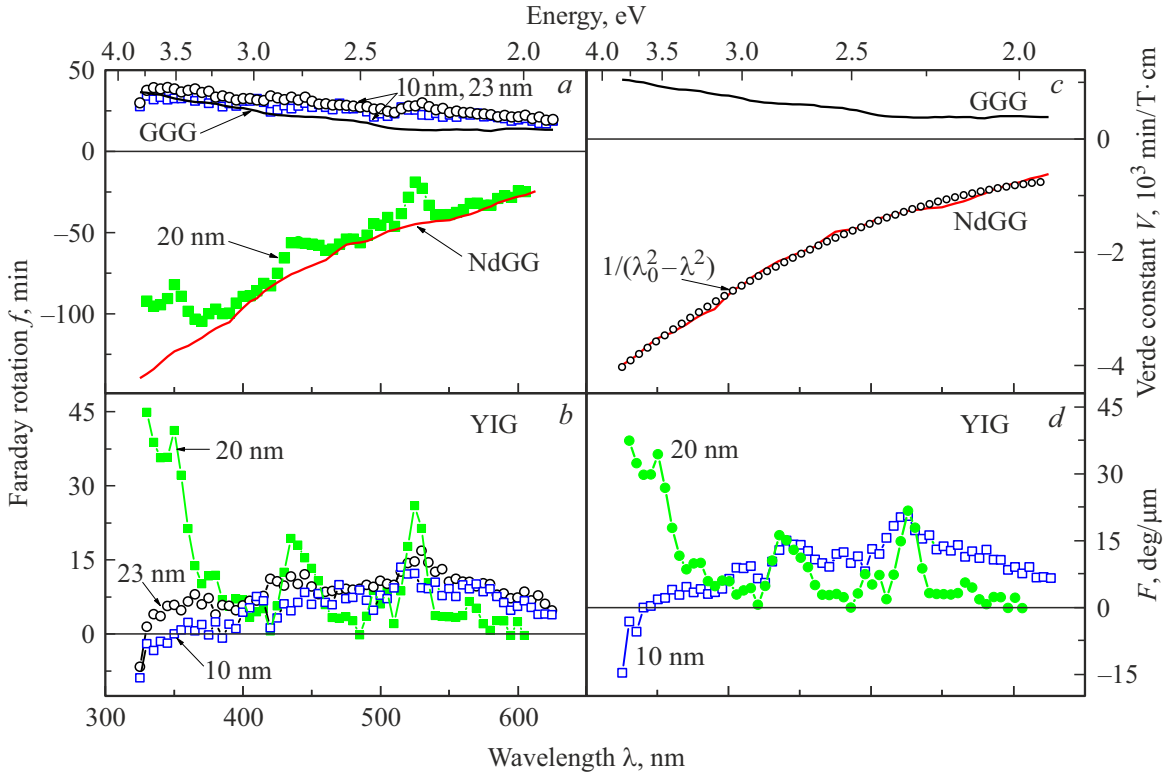

Figure 2. (a) Faraday effect spectra (f) for the GGG and NdGG substrates (solid line), YIG/GGG structures with the film thickness $d = 10$ nm, $d = 23$ nm and YIG/NdGG with $d = 20$ nm at $H = 0.7$ T. (b) Spectra f for the YIG films less the contribution of a particular substrate. (c) Verdet constant spectra (V) for the GGG and NdGG substrates, symbols — treatment using the equation $1/(\lambda_0^2 - \lambda^2)$. ($d$) Specific Faraday effect spectra (F) for the $d = 10$ nm and $d = 20$ nm films at $H = 0.7$ T.

types of substrates: GGG and NdGG. The Faraday effect provides direct information on the bulk magnetic properties of the YIG/GGG and YIG/NdGG structures, while the Kerr effect reflects magnetic properties of the surface.

Figure 2 shows the Faraday effect spectra $f(\lambda)$ for the YIG/GGG, YIG/NdGG structures and single-crystalline GGG, NdGG substrates. For ease of analysis, the figure also shows the spectra $f(\lambda)$ for the YIG films measured after subtracting the substrate contribution. Experimental data comparison shows that $f(\lambda)$ in bulk substrates is greater or comparable with that in the nanoscale YIG films. For substrates, the Faraday effect has a different sign and increases with decreasing the wavelengths, (Figure 2, a), which corresponds to the existing data on the study of the Faraday effect in rare-earth ions [4,18]. This feature also appeared in the short-wavelength range of the Faraday effect spectra in the YIG films (Figure 2, b, d). Fine structure of the spectra $f(\lambda)$ for NdGG was described in [8,9], where it is associated with the 5d-transitions $4f^3 \rightarrow 4f^2$ in the Nd^{3+} rare-earth ions. Only a smeared peak was observed in our case, which is associated with a relatively wide interval of optical spectral measurements ($\Delta\lambda = 10$ nm).

Figure 2, c and d shows the Verdet constant spectra $V = f/(Hd)$ for the substrates and specific Faraday rotation (F) for the films. For the GGG substrate, the constant V demonstrates a near-linear growth from +428 to +1048 min/(T·cm) in the range from $\lambda = 620$ nm (2 eV) to $\lambda = 320$ nm (3.9 eV) (Figure 2, c). This data agrees with [7,11,19], where it was shown that the Verdet constant for GGG achieves its highest value within the region of resonance transition at $\lambda_0 = 153$ nm [11]. For the NdG substrate, V is negative and increases from −560 to −4000 min/(T·cm) in the same spectral range (Figure 2, c) as in [8,20]. Rough estimate of λ_0 using the expression $1/V = \text{const}(\lambda_0^2 - \lambda^2)$ gives $\lambda_0 \sim 240$ nm, which is close to the $^4I_{9/2} \rightarrow {}^4P_{1/2}$ type intracenter transitions between the Stark levels of Nd^{3+} [21]. Note that the Verdet constant for the NdGG substrate is almost twice as high as that for GGG, which may be caused by the proximity of the λ_0 value and by the influence of the field on the magnetic sublattice with the Nd^{3+} ions [14,20].

The presence of a positive Faraday effect in the YIG films leads to the increase in the total Faraday effect in the YIG/GGG structure and, on the contrary, decrease in the YIG/NdGG structure. Note that the double increase in the film thickness is accompanied by a proportional effect enhancement (Figure 2). It is known that the specific Faraday rotation $F(\lambda)$ for high quality magnetic films should be the same regardless of their thickness or type of substrate. In our case, Figure 2, d demonstrates that the obtained

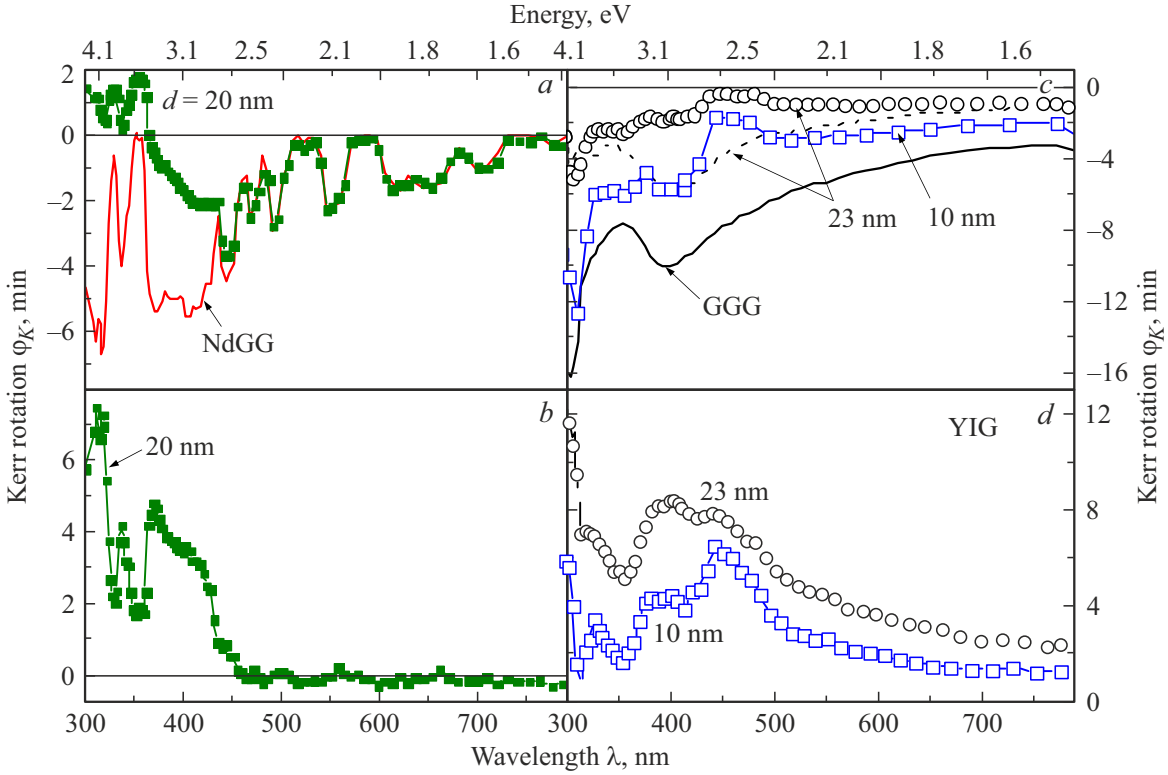

Figure 3. (a) The polar Kerr effect spectra (φ_K) for the YIG/NdGG structure with film with $d = 20$ nm and for the NdGG substrate at $H = 0.4$ T. (b) φ_K spectrum for the YIG film $d = 20$ nm less the paramagnetic contribution of the NdGG substrate. (c) φ_K spectra for the YIG/GGG structures with film $d = 23$ nm and 10 nm and the GGG substrate at $H = 0.4$ T. The Kerr effect spectrum for YIG/GGG with film $d = 23$ nm measured on the film side is shown by dashed line. (d) φ_K Spectra for the YIG films with $d = 23$ nm and 10 nm after subtraction of the GGG substrate contribution.

values of $F(\lambda)$ for the nanoscale YIG films on various substrates are close to each other. An important result is also that the maximum specific Faraday rotations F in the ultra-thin films achieve almost 20 deg/μm (Figure 2, d), which is only approximately twice as low as in the best YIG single-crystal samples [22] and 6 times as high as in the epitaxial YIG layers grown by the standard liquid-phase epitaxy method [20]. This indicates the high MO quality of our thin-film samples obtained by the laser ablation.

YIG films feature two intense bands in the spectra $F(\lambda)$ at $\lambda_1 \sim 430$ nm (2.9 eV) and $\lambda_2 \sim 520$ nm (2.4 eV) close to the data in [22,23]. It is known from the literature that a band at λ_1 is associated with parity-forbidden transitions from $t_{1g}(\pi)$- to $t_{2g}(\pi)$-states of the Fe^{3+}–O^{2-} complexes in the octahedral lattice , and a band at λ_2 is associated with the d–d-transitions in the Fe^{3+} ions in the tetrahedral sublattice [21,23,24]. It is known that in the Faraday effect spectra for YIG a change in the sign should be observed at $\lambda \sim 350$ nm (~ 3.5 eV) [20,24]. Similar behavior was recorded only in the YIG/GGG structure (Figure 2, b and d), while for YIG/NdGG only a monotonic growth of $F(\lambda)$ without change of sign was observed.

To assess the effect of the relaxation layer formed at the film/substrate interface due to discrepancy (mismatch) of $f_c = (a - b)/a$ in the crystal lattices of the film (a) and substrate (b) on the MO properties of films, critical film thickness h/a was calculated. In the first approximation, when the lattice constants of the film and substrate differ negligibly, h/a can be derived from the equation proposed in [6]:

$$\ln[2\pi f_c e/(1-\sigma)] + 4\pi(1-\sigma)^2 h f_c/[(1-2\sigma)a] = 0, \quad (3)$$

where σ is Poison's ratio (for our case $a = 0.3$ [6]), $f_c = 0.001$ for YIG/GGG and $f_c = 0.014$ for YIG/NdGG.

From expression (3) it follows that $h/a \sim 20$ for the YIG/GGG structure , and $h/a \sim 5$ for YIG/NdGG. Stresses and high density of displacement dislocations in the relaxation layer lead to deformation and failure of the YIG sublattices in the film/substrate interface and, consequently, to decrease in the Faraday effect in films thinner than ~ 25 nm for the YIG/GGG structure. However, this is not clearly evident in the experiment (Figure 2, d), which possibly requires a separate examination of a set of YIG films of different thicknesses (higher and lower h/a) and/or more accurate assessment of h/a.

Thus, the nanoscale YIG films close to and lower than the critical thickness demonstrate the same specific Faraday rotation as the bulk YIG crystals.

Kerr effect in the nanoscale YIG films and GGG, NGG substrates

The polar Kerr effect spectrum shown in Figure 3, *a* for the double-side-polished NdGG-substrate can be reasonably associated with the interference of reflected light as in [25]. However, when analyzing the $\varphi_K \sim 1/\lambda$ type dependence (not shown), there is no band periodicity in the φ_K spectrum. Thus, intense peculiarities in the φ_K spectrum may be associated only with the intracenter electronic transitions in $Nd_3Ga_5O_{12}$ that were discussed in detail in [13,21]. It is important to emphasize that after subtracting φ_K the NdGG substrate contribution from the YIG/NdGG spectrum, a film spectrum was obtained (Figure 3, *b*) that resembled the polar Kerr effect spectrum in the bulk YIG polycrystals and single crystals [26,27]. The film spectrum has pronounced bands with peaks at $E_1 \sim 4$ eV and $E_2 \sim 3.4$ eV associated with the electrodipole transitions in the octahedral sublattice from the $2p$-oxygen states to the t_{1g} and t_{2g} spin-orbit split $3d$-states of the Fe^{3+} ions. Singularities of $\varphi_K(\lambda)$ at $\lambda = 330$ nm (3.8 eV) and 354 nm (3.5 eV) are likely attributed to the appearance of optical properties of the NdGG substrate (Figure 3, *a* and *b*).

In the GGG substrate, the negative $\varphi_K(\lambda)$ is substantially higher than in NdGG, and grows quickly as the wavelength decreases (Figure 3, *c*). The influence of the substrate on the behavior of the Kerr effect is clearly seen from a comparison of the spectral curves $\varphi_K(\lambda)$ for the YIG/GGG structure obtained with light incident from the film side and from the substrate side (Figure 3, *c*). Figure 3, *d* shows the φ_K spectra for the nanoscale YIG films recorded after subtracting the additive contribution of the paramagnetic GGG substrate from the YIG/GGG spectra. Note that the effect becomes positive throughout the spectral range and the shape of spectra agrees with the experimental and calculated data for YIG [26–28]. It can also be noted that the change of sign of the effect disappears (Figure 3, *b*) due to occurrence of an intense positive background at $\lambda > 400$ nm ($E < 3$ eV). The origin of such spectral shift is most probably associated with the influence of the substrate as well as the enhancement of low-energy transitions between the crystal-field-split $3d$-states of the Fe^{3+} ions in the octahedral and tetragonal sublattices in the film relaxation layer [1].

A substantial contribution of the light reflected from the substrate to the magnetoabsorption (magnetotransmission) effect in doped lanthanum manganite films has been also noted earlier [29]. Contribution of the Faraday effect to the absorption of nonpolarized light in a $CoFe_2O_4$ single crystal was also estimated [30]. The authors of [13] has also indicated a possible impact of the Faraday rotation on the Kerr effect spectrum of the YIG film in the YIG/NdGG structure. The experimental data we obtained on the transmission and reflection of light allows us, in a first approximation, to directly assess the additive contribution of the Faraday effect to the Kerr effect (Fig. 4) for YIG films taking into account the angle of incidence and the double passage of light in the thickness of the film due to its reflection from the boundary of the film/substrate. As shown in the figure, after subtraction of the Faraday effect, the φ_K spectrum changes substantially: bands appear at $\lambda = 430$ nm (2.9 eV) and $\lambda = 520$ nm (2.4 eV). However, the effect is still negative and achieves up to -30 min, which exceeds greatly the known experimental and calculated data [1,13,24–28]. Thus, the Faraday rotation contribution to the polar Kerr effect spectra or the YIG/substrate structures may occur, however, its quantitative estimation is hindered. It is known that in case of a diffusely reflective surface, contributions associated with the back-reflected light (the Faraday effect, ellipticity, etc.) may be excluded from the φ_K spectra of the YIG films. To check this assumption, detailed studies of films grown on double-side-polished substrates as well as on substrates with rough back side shall be conducted in the transmitted and reflected light, which is beyond the scope of this study.

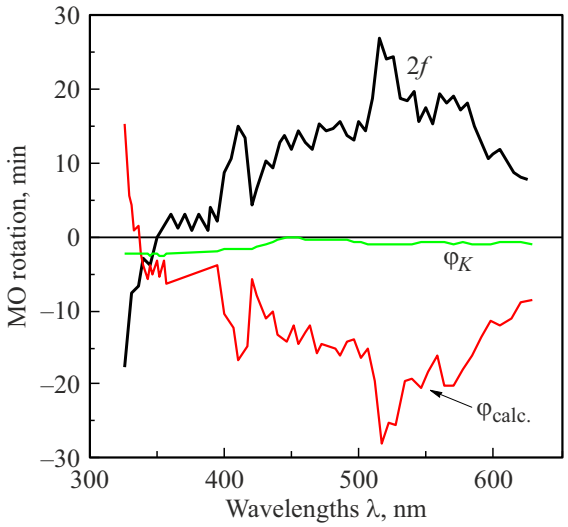

Figure 4. Experimentally obtained spectral dependences of the Kerr effect and doubled Faraday effect ($2f$) for the YIG film with $d = 23$ nm and calculated Kerr effect spectrum (φ_{calc}).

Field dependences of the MO effects in the YIG films and GGG, NGG substrates

As shown above, the nanoscale films have the MO properties similar to those of bulk YIG. The insets in Figure 5 show the field dependences of the Verdet constant $V(H)$ and Kerr effect for the GGG and NdGG substrates in field up to 1 T. Curves $V(H)$ and $\varphi_K(H)$ demonstrate the linear dependence typical of paramagnetic materials without saturation [13,17,31], but with opposite signs and different slope of the curve. Note that values of V and φ_K for NdGG are much higher than for GGG, which, according to the authors of [30], is attributed to the effect of magnetic field on the NdGG magnetic sublattices.

Figure 5, *a* and *b* shows the field dependences of the Faraday effect $f(H)$ and Kerr effect $\varphi_K(H)$ for the YIG

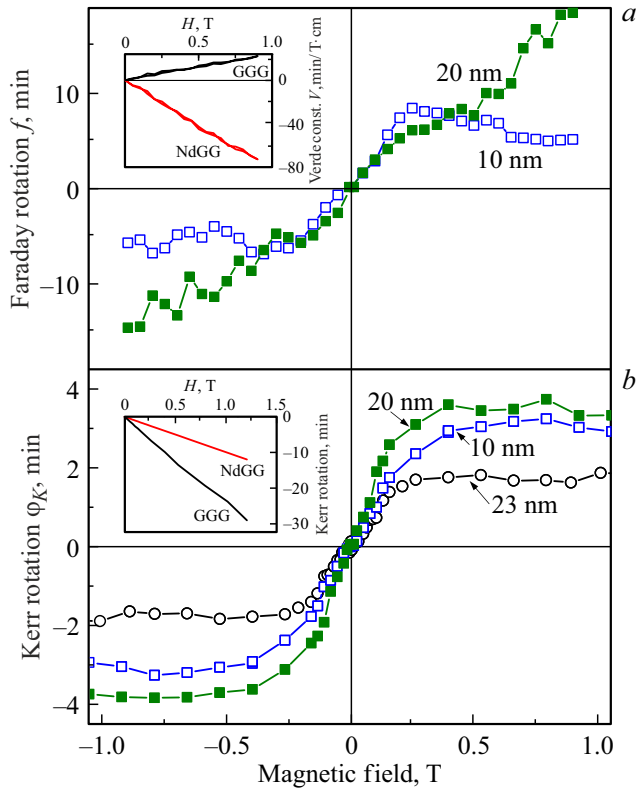

Figure 5. (a) Field dependences of the Faraday effect (f) for the YIG films with $d = 10$ nm and 20 nm at $\lambda = 390$ nm (3.2 eV) less the substrate contribution. The inset shows H vs. the Verdet constant (V) for the GGG and NdGG substrates at $\lambda = 350$ nm (3.5 eV). (b) Field dependences of the polar Kerr effect (φ_K) for the YIG films with $d = 23$ nm t $\lambda = 350$ nm (3.5 eV), $d = 10$ nm at $\lambda = 400$ nm (3.1 eV) and $d = 20$ nm at $\lambda = 440$ nm (2.8 eV) less the paramagnetic contribution from the corresponding substrate. The inset shows the field dependences of the Kerr effect for the GGG and NdGG substrates at $\lambda = 400$ nm.

films plotted after subtracting the substrate contribution to the Faraday effect in the YIG/substrate structures. Note that, due to the significant substrate contribution in the short-wavelength region, the field dependences $f(H)$ in the samples were measured in the vicinity of their maximal values at $\lambda \geq 350$ nm (~ 3.5 eV) (Figure 3). However, it was not always possible to identify the Faraday effect in a nanoscale film. For example, for the 20 nm YIG/NdGG film, just a weak kink was recorded in the curve $f(H)$ accompanied by further linear growth at the chosen wavelength, which is probably attributed to the effect of the substrate's Faraday rotation (Figure 2, c). For other GGG-based films the field dependence of $f(H)$ follows magnetization behavior typical for ferromagnetic materials and saturate in the field $H_S \sim 0.2$ T.

Unlike the Faraday effect, the saturation field H_S in the Kerr effect almost does not depend on the film thickness and type of substrate (Figure 5, b). The form of curves $\varphi_K(H)$ for all studied nanoscale films is defined by their field dependences of magnetization. Minor deviation of the effect's magnitude and saturation field values for films from the known literature data may be attributed to different quality of the studied samples, shape anisotropy, and difficulties in accounting for the substrate contribution. For example, for the YIG/NdGG structure, reduction of H_S to ~ 0.17 T corresponds to the negative contribution of magnetic anisotropy ($H_a \sim 0.1$ T [10,32]) that facilitates orientation of the magnetic moment normal to the film surface.

Conclusion

The fabricated thin-film structures in the form of nanoscale 10, 20 and 23 nm $Y_3Fe_5O_{12}$ films deposited by the laser molecular beam epitaxy method on dielectric substrates made of gadolinium-gallium garnet, $Gd_3Ga_5O_{12}$, and neodymium-gallium garnet, $Nd_3Ga_5O_{12}$, demonstrate high structural perfection and MO quality typical of $Y_3Fe_5O_{12}$ bulk films, single crystals and polycrystals. The peak of specific Faraday rotation of films was 15–20 deg/μm and the polar Kerr effect was approx. 5–10 min. Field dependences of the Faraday effect in the films demonstrate saturation in fields ~ 0.2 T at wavelengths greater than 350 nm. For shorter wavelengths, there is strong paramagnetic contribution of substrates. At the same time, the saturation field in the Kerr effect negligibly depends on the film thickness and type of substrate.

It is shown that the Faraday- Kerr effects in the $Y_3Fe_5O_{12}$ films are lower or comparable with the those for the $Gd_3Ga_5O_{12}$ and $Nd_3Ga_5O_{12}$ substrates. The Verdet constants obtained for the substrates are equal to $+1048$ min/(T·cm) for $Gd_3Ga_5O_{12}$ and -4000 min/(T·cm) for $Nd_3Ga_5O_{12}$ at $\lambda = 320$ nm.

The thickness of the relaxation layer formed in the films (h/a) due to discrepancy of the lattice parameters in film and substrate are estimated to be equal to $h/a \sim 20$ for the $Y_3Fe_5O_{12}/Gd_3Ga_5O_{12}$ structure and $h/a \sim 5$ for $Y_3Fe_5O_{12}/Nd_3Ga_5O_{12}$. Nevertheless, even the films with near-critical thickness can have the specific Faraday rotation close to that in the $Y_3Fe_5O_{12}$ single crystals and polycrystals.

Thus, the ultra-thin $Y_3Fe_5O_{12}$ films synthesized by the laser molecular beam epitaxy method and having low absorption of light and high Faraday and Kerr effects may be of interest for creating MO-active nanostructures and planar optoelectronic components based on them.

Funding

This study was carried out under the state assignment of the Ministry of Science and Higher Education of the Russian Federation (theme „Spin“ № 122021000036-3).

Conflict of interest

The authors declare that they have no conflict of interest.

References

[1] A.K. Zvezdin, V.A. Kotov. Modern magnetooptics and magnetooptical materials (Institute of Physics Publishing: Bristol, Philadelphia, USA, 1997), p. 381. DOI: 10.1887/075030362x.

[2] B.J.H. Stadler, T. Mizumoto. IEEE Photonics Journal, **6** (1), 0600215 (2014). DOI: 10.1109/JPHOT.2013.2293618

[3] S. Kharatian, H. Urey, M. Onbasli. Adv. Optical Mater., 19013481 (2019). DOI: 10.1002/adom.201901381

[4] V.B. Novikov, A.M. Romashkina, T.V. Murzina, D.A. Ezenkova, I.A. Rodionov, K.N. Afanas'ev, A.V. Baryshev. Opt. Spectr. **128** (9), 1481 (2020)
DOI: 10.1134/S0030400X20090155.

[5] V.A. Kotov, V.G. Shavrov, A.F. Popkov, M. Vasiliev, K. Alameh, M. Nur-E-Alam, L.N. Alyabyeva, D.E. Balabanov, V.I. Burkov, M.K. Virchenko. J. of Nanomaterials, 7605620 (2018). DOI: 10.1155/2018/7605620

[6] J.H. Van der Merwe. *Lattice mismatch and bond strength at the interface between oriented films and substrates* (Pergamon Press, Oxford, London, New York, Paris, 1964) p. 172.

[7] V. Berzhansky, T. Mikhailova, A. Shaposhnikov, A. Prokopov, A. Karavainikov, V. Kotov, D. Balabanov, V. Burkov. Appl. Opt., **52** (26), 6599 (2013). DOI: 10.1364/AO.52.006599

[8] S.M. Suturin, A.M. Korovin, V.E. Bursian, L.V. Lutsev, V. Bourobina, N.L. Yakovlev, M. Montecchi, L. Pasquali, V. Ukleev, A. Vorobiev, A. Devishvili, N.S. Sokolov. Phys. Rev. Mat., **2**, 104404 (2018). DOI: 10.1103/PhysRevMaterials.2.104404.

[9] A.K. Zvezdin, S.V. Koptsik, G.S. Krinchik, R.Z. Levitin, V.A. Lyskova, A.I. Popov. JETP Lett., **37** (7), (1983).

[10] K.M. Mukimov, B.Yu. Sokolov, U.V. Valiev. Phys. Stat. Sol. (a), **119** (1), 307 (1990). DOI: 10.1002/pssa.2211190136

[11] M. Guillot, X. Wei, D. Hall, Y. Xu, J.H. Yang, F. Zhang. J. Appl. Phys., **93** (10), 8005 (2003). DOI: 10.1063/1.1558086

[12] P. Novotn., M. Křižánková, P. Boháček. J. Analytical Sciences, Methods and Instrumentation, **3**, 13 (2013).
DOI: 10.4236/jasmi.2013.31003

[13] N.S. Sokolov, V.V. Fedorov, A.M. Korovin, S.M. Suturin, D.A. Baranov, S.V. Gastev, B.B. Krichevtsov, K.Yu. Maksimova, A.I. Grunin, V.E. Bursian, L.V. Lutsev, M. Tabuchi. J. Appl. Phys., **119**, 023903 (2016). DOI: 10.1063/1.4939678

[14] B.B. Krichevtsov, A.M. Korovin, S.M. Suturin, A.V. Telegin, I.D. Lobov, N.S. Sokolov. Thin Solid Films, **756**, 139346 (2022). DOI: 10.1016/j.tsf.2022.139346

[15] B.B. Krichevtsov, S.V. Gastev, S.M. Suturin, V.V. Fedorov, A.M. Korovin, A.G. Bursian, M.P. Banshchikova, M. Volkova, V.E. Tabuchi, N.S. Sokolov. Science and Technology of advanced Materials, **18** (1), 351 (2017).
DOI: 10.1080/14686996.2017.1316422

[16] T. Yoshimoto, T. Goto, K. Shimada, B. Iwamoto, Y. Nakamura, H. Uchida, C.A. Ross, M. Inoue. Adv. Electron. Mater., **4** (7), 1800106 (2018). DOI: 10.1002/aelm.201800106

[17] F.F. Sizov, Yu.I. Ukhanov. *Magneto-optical Faraday and Voigt effects as applied to semiconductors.* (Naukova Dumka, Kiev, 1979) [in Russian].

[18] N.F. Borrelli. J. Chem. Phys., **41** (11), 3289 (1964).
DOI: 10.1063/1.1725727

[19] M. Sabbaghi, G.W. Hanson, M. Weinert, F. Shi, C. Cen. J. Appl. Phys., **127**, 025104 (2020). DOI: 10.1063/1.5131366

[20] W. Wang. J. Appl. Phys., **102**, 063905 (2007).
DOI: 10.1063/1.2781525

[21] V.V. Randoshkin, N.V. Vasil'eva, V.G. Plotnichenko, Yu.N. Pyrkov, S.V. Lavrishchev, M.A. Ivanov, A.A. Kiryukhin, A.M. Saletskii, N.N. Sysoev, Phys. Solid State, **46**, 1030 (2004). DOI: 10.1134/1.1767239

[22] W. Wettling, B. Andlauer, P. Koidl, J. Schneider, W. Tolksdor. Phys. Status Solidi B, **59**, 63 (1973).
DOI: 10.1002/pssb.2220590105

[23] G.B. Scott, D.E. Lacklison, H.I. Ralph, J.L. Page. Physical Review B, **12** (7), 2562 (1975). DOI: 10.1103/PhysRevB.12.2562

[24] B. Andlauer, J. Schneider, W. Wettling. Appl. Phys., **10**, 189 (1976). DOI: 10.1007/BF00897217

[25] S. Sumi, H. Awano, M. Hayashi. Scientific Reports, **8** (1), 776 (2018). DOI: 10.1038/s41598-017-18794-w

[26] S. Visnovsky, V. Prosser, R. Krishnan, V. Parizek, K. Nitsch, L. Svobodova. IEEE Trans. magn., **17** (6), 3205 (1981). DOI: 10.1109/TMAG.1981.1061610

[27] S. Visnovsky, R. Krishnan, V. Prosser. J. Appl. Phys., **49**, 2212 (1978). DOI: 10.1063/1.324734

[28] W.K. Li, G.Y. Guo. Physical Review B, **103** (1), 014439 (2021). DOI: 10.1103/PhysRevB.103.014439

[29] Yu.P. Sukhorukov, A.V. Telegin, A.B. Granovskii, E.A. Gan'shina, S.V. Naumov, N.V. Kostromitina, L.V. Elokhina, J. Gonzalez. JETP., **111** (3), 353 (2010).
DOI: 10.1134/S1063776110090037.

[30] Yu. Sukhorukov, A. Telegin, N. Bebenin, V. Bessonov, S. Naumov, D. Shishkin, A. Nosov. Magnetochemistry, **8**, 135 (2022). DOI: 10.3390/magnetochemistry8100135

[31] O.A. Petrenko, D. McK Paul, C. Ritter, T. Zeiske, M. Yethiraj. Physica B, **266**, 41 (1999). DOI: 10.1088/1742-6596/145/1/012026

[32] B.B. Krichevtsov, V.E. Bursian, S.V. Gastev, A.M. Korovin, L.V. Lutsev, S.M. Suturin, K.V. Mashkov, M.P. Volkov, N.S. Sokolov. arXiv:1901.10800v1 [cond-mat.mes-hall].
DOI: 10.48550/arXiv.1901.10800

Translated by E.Ilinskaya